

# Minimum-phase signal calculation using the real cepstrum

Adrian D. Smith, Robert J. Ferguson

## ABSTRACT

The concept of minimum phase in geophysics is an important one, especially for processes such as statistical deconvolution which assume the condition in the source wavelet. We wish to have an alternative method to the Hilbert transform to convert a signal of arbitrary phase to its minimum phase equivalent, while retaining the same amplitude spectrum. We implement a minimum-phase reconstruction based on the real cepstrum developed for a finite-impulse response (FIR) filters by treating the signal as a filter. We demonstrate that the algorithm is able to handle signals with ill-conditioned amplitude spectra and still give minimum-phase outputs through analysis of pole-zero plots, along with a simple deconvolution test. We also introduce two metrics: the Pole-Zero Ratio (PZR) and Pole-Zero Distance (PZD) as potential quantitative descriptions of how close a signal is to being minimum phase.

## INTRODUCTION

The concept of minimum phase signals plays a very important role in seismic data processing. One particular class of processing algorithms requiring the seismic source signature under study be minimum phase are statistical or "blind" deconvolution methods, both stationary (Robinson, 1967; Robinson and Treitel, 1967) and non-stationary (Margrave et al., 2011). These processes are based on the convolutional model of the Earth, whereby a source wavelet is convolved with a reflectivity function to generate a recorded seismic trace (Yilmaz, 2001). Deconvolution aims to remove the signature of the source from the trace, leaving reflectivity. This reflectivity represents subsurface structure - the imaging of which is the goal of seismic reflection surveys.

The definition of "minimum phase" or "minimum phase delay" comes originally from filtering theory in digital signal processing (Lamoureux et al., 2011). The classical mathematical definition of a minimum-phase *system* is one where all of the poles and zeroes of its rational transfer function in the Z-transform domain lie inside the unit circle on the complex plane (Karl, 1989; Oppenheim and Schaffer, 2009). There is a discrepancy between this definition and the definition used in geophysics, which is that minimum-phase filters/systems have poles and zeroes *outside* the unit disk (Lamoureux and Margrave, 2007a; Lamoureux et al., 2011). This is due to the difference in the definition of the powers of  $z$  in the Z-transform (Margrave, 2013). We use the classic definition in this report.

The definition of a minimum-phase *signal* is physical in nature, defined as a signal where the energy in the signal is concentrated near the front of the signal (Lamoureux et al., 2011). This definition is useful for seismic processing, as experimentation has shown that impulsive seismic sources, dynamite for example, have this property (Sherwood and Trorey, 1965; Ziolkowski and Bokhorst, 1993). We cannot use the classical *system* definition of poles and zeroes to precisely describe minimum-phase *signals*, as one cannot assume the spectra of general signals are always well-represented by rational functions (Lamoureux and Margrave, 2007a). Also, real signals are bandlimited, with an assumed

amplitude spectrum outside that range to be zero. This causes computational issues when calculating a minimum-phase equivalent using pre-existing methods (Lamoureux and Margrave, 2007a). We propose however to think of *signals* as digital filters, classify them as mixed or minimum phase using the classic definition of poles and zeroes. While inaccuracies may be introduced by doing so, we feel that using the poles and zeroes of a signal is useful, especially in cases where we want to describe how "close" a signal is to being minimum phase and how that may impact processing results, such as deconvolution.

## Motivation

Although we do not have direct control over seismic sources to ensure that they generate a mathematically perfect minimum-phase source, the assumption seems to hold well enough with seismic data in order for deconvolution to work (Ziolkowski and Bokhorst, 1993). However there are other datasets based on measuring reflected electromagnetic radiation that are similar to seismic in nature, both geophysical such as in georadar (GPR) (Jol, 2008; Gurbuz et al., 2009), and medical imaging (Fear et al., 2002; Bourqui et al., 2012), where we in theory have better control over the source. Should we want to use seismic-based processing methods requiring a minimum-phase source, we need to be able to precondition a source pulse in order to generate the desired source wavelet. At some point, we would require the ability to convert an arbitrary mixed-phase wavelet to a minimum phase equivalent, with the same amplitude spectrum. This is because such radar signals tend to be defined only in terms of their desired amplitude spectrum characteristics, with little concern given to phase.

Lamoureux and Margrave (2007c) and Lamoureux and Margrave (2007b) describe methods and give examples of computing more generally the minimum phase version of any band-limited signal using a stable criteria, using truncation of infinite-impulse response (IIR) filters. In this report, we aim to accomplish two things: 1) implement and test an alternative algorithm to convert a signal to its minimum phase equivalent and 2) introduce simple metrics for quantifying the "minimum phaseness" of a signal.

The algorithm we implement was developed by Pei and Lin (2006) as a method to design an arbitrary length minimum-phase finite-impulse response (FIR) filter from a mixed-phase input. It allows us to calculate the minimum-phase equivalent sequence of an arbitrary mixed-phase input with the output having the same amplitude spectrum of the input. This algorithm has several advantages over other ones:

- The difficulty of root finding (especially in high-order filters) such as in the method of Herrmann and Schuessler (1970) is avoided. This allows us to calculate the minimum-phase equivalent of longer input signals than other methods.
- The cumbersome process of phase unwrapping as required in the method of Mian and Nainer (1982) is avoided.
- A similar method developed Stathaki and Fotinopoulos (2001) requires that the input be linear-phase, while the input for the method under investigation (Pei and Lin, 2006) can be of general mixed-phase.

The algorithm extends from the previous work of Mian and Nainer (1982) and avoids the phase unwrapping problem by using the real cepstrum (Pei and Lin, 2006). The method requires only two fast Fourier transforms (FFT)'s and a recursive procedure to find the minimum-phase equivalent of a signal from its real cepstrum. Although this algorithm is designed for sequences/filters, signals under study are represented as discrete signals, and as such we apply the reconstruction algorithm to them.

We now cover several important points concerning the cepstrum and how they relate to the algorithm designed by Pei and Lin (2006), which we give the name *minrceps*. We then describe the algorithm itself and provide examples of the performance of the minrceps algorithm using both pole-zero plots and a simple deconvolution test. To conclude, we attempt to quantify the degree of a signal's "minimum phaseness", and what that implies for the accuracy of geophysical processes relying on the minimum-phase source assumption, such as deconvolution.

### THE CEPSTRUM

The *power cepstrum* of a signal was defined in Bogert et al. (1963) as the squared magnitude of the inverse Fourier transform of the natural logarithm of the squared magnitude of the Fourier transform of a signal. This is given as follows:

$$PC = |\mathcal{F}^{-1}\{\ln |\mathcal{F}\{x(n)\}|^2\}|^2, \quad (1)$$

where  $PC$  denotes the power cepstrum,  $x(n)$  is a real sequence,  $\ln$  the natural logarithm, and  $\mathcal{F}$  and  $\mathcal{F}^{-1}$  denote forward and inverse Fourier transforms respectively. Let  $X(e^{i\omega})$  represent the Fourier transform of  $x(n)$ .

From this, the sequence's complex cepstrum  $\hat{c}(n)$  and its real cepstrum  $\hat{h}(n)$  can be defined as

$$\begin{aligned} \hat{C}(e^{i\omega}) &= \ln [X(e^{i\omega})] \\ &= \ln \left[ |X(e^{i\omega})| e^{i \arg[X(e^{i\omega})]} \right] \\ &= \ln |X(e^{i\omega})| + i \arg[X(e^{i\omega})] \end{aligned} \quad (2)$$

$$\hat{H}(e^{i\omega}) = \text{Re}\{\hat{C}(e^{i\omega})\} = \ln |X(e^{i\omega})| \quad (3)$$

$$\hat{c}(n) = \mathcal{F}^{-1}\{\hat{C}(e^{i\omega})\} \quad (4)$$

$$\hat{h}(n) = \mathcal{F}^{-1}\{\hat{H}(e^{i\omega})\} \quad (5)$$

(Oppenheim, 1965). Note in Equations 2 and 4 when calculating the complex cepstrum, we need to compute the natural logarithm of a complex number. The imaginary part of the complex logarithm must be continuous and without linear-phase term to avoid ambiguity (Pei and Lin, 2006).

### Minimum/maximum phase sequences and their complex cepstra

There are two useful properties from Oppenheim and Schaffer (2009) that can be used to describe the special relationship between minimum and maximum phase sequences and their complex cepstra:

1. If  $x(n)$  is a *minimum-phase sequence*, its complex cepstrum  $\hat{c}(n)$  will be a *causal sequence* - that is,  $\hat{c}(n) = 0$  for  $n < 0$ .
2. If  $x(n)$  is a *maximum-phase sequence*, its complex cepstrum  $\hat{c}(n)$  will be an *anti-causal sequence* - that is,  $\hat{c}(n) = 0$  for  $n > 0$ .

### Relationship between minimum-phase sequence and its complex cepstrum

An arbitrary sequence  $x(n)$  and its complex cepstrum  $\hat{c}(n)$  are related by an implicit recursive relation from Oppenheim and Schaffer (2009) as

$$x(n) = \begin{cases} e^{\hat{c}(0)}, & \text{if } n = 0 \\ \sum_{k=-\infty}^{\infty} \binom{k}{n} \hat{c}(k)x(n-k) & \text{if } n \neq 0 \end{cases} \quad (6)$$

From this, if  $x(n)$  is a finite minimum-phase sequence, the summation in Equation 6 is reduced to finite terms as

$$x(n) = \begin{cases} e^{\hat{c}(0)} & \text{if } n = 0 \\ \sum_{k=0}^n \binom{k}{n} \hat{c}(k)x(n-k) & \text{if } n > 0 \end{cases} \quad (7)$$

### Reconstruction of a causal sequence from its even part

If  $x(n)$  is a causal sequence and  $x_e(n) = [x(n) + x(-n)]/2$  is the even part of  $x(n)$ , then  $x(n)$  can be recovered from  $x_e(n)$  as

$$x(n) = x_e(n)u_+(n), \quad \text{where } u_+(n) = \begin{cases} 0 & \text{if } n < 0 \\ 1 & \text{if } n = 0 \\ 2 & \text{if } n > 0 \end{cases} \quad (8)$$

(Pei and Lin, 2006).

### Fourier transform pair between time and frequency domain

Let  $x_e(n)$  and  $x_o(n)$  be the even and odd parts of a sequence  $x(n)$  respectively. If we take the real and imaginary parts of the Fourier transform of  $x(n)$ , we have the following relations:

$$x_e(n) = \mathcal{F}^{-1}\{\text{Re}[X(e^{i\omega})]\} \quad (9)$$

$$x_o(n) = \mathcal{F}^{-1}\{i\text{Im}[X(e^{i\omega})]\} \quad (10)$$

(Pei and Lin, 2006).

### Relationship between complex cepstrum and real cepstrum

If  $x(n)$  is a real-valued sequence, its corresponding complex cepstrum is also real-valued according to the recursive relation given in Equation 6. As this assumption holds true for the most part, we denote  $\hat{c}_e(n)$  as the even part of  $\hat{c}(n)$  - which is the complex cepstrum of  $x(n)$ . If we substitute  $X(e^{i\omega})$  with  $\hat{C}(e^{i\omega}) = \ln[X(e^{i\omega})]$  into Equation 9 we get:

$$\hat{c}_e(n) = \mathcal{F}^{-1}\{\text{Re}[\hat{C}(e^{i\omega})]\} = \mathcal{F}^{-1}\{\ln|X(e^{i\omega})|\} \quad (11)$$

Continuing, we use the definition of the real cepstrum in (3) and (5), we get

$$\hat{c}_e(n) = \mathcal{F}^{-1}\{\hat{H}(e^{i\omega})\} = \hat{h}(n) \quad (12)$$

This result shows that the real cepstrum  $\hat{h}(n)$  is actually the even part of the complex cepstrum  $\hat{c}(n)$  (Benesty et al., 2008).

The properties discussed throughout this section are required for the development of the minrceps algorithm. We now describe implementation of the algorithm.

### IMPLEMENTATION OF MINRCEPS ALGORITHM

The properties of the cepstrum mentioned in the previous section section to construct a minimum-phase sequence. Given a mixed-phase real valued input signal  $x(n)$ , we want to generate a signal  $x_{min}(n)$  which is minimum phase and has the same amplitude spectrum as the input

$$|X_{min}(e^{i\omega})| = |X(e^{i\omega})|. \quad (13)$$

Since the real cepstrum is uniquely determined by the magnitude component of a sequence's frequency response (Relations 3, 5 and 13), two sequences with the same amplitude spectra must have the same real cepstra (Benesty et al., 2008; Pei and Lin, 2006). Therefore,

$$\hat{h}(n) = \hat{h}_{min}(n). \quad (14)$$

Recall from earlier,  $\hat{c}_{min}(n)$  is a causal sequence and  $\hat{h}_{min}(n)$  is the even part of  $\hat{c}_{min}(n)$  (Benesty et al., 2008). We can use this relationship and equation 8 to reconstruct  $\hat{c}_{min}(n)$  from  $\hat{h}_{min}(n)$ . After we have found  $\hat{c}_{min}(n)$ , we can get  $x_{min}(n)$  from equation 7 (Oppenheim and Schaffer, 2009).  $x_{min}(n)$  represents the minimum-phase sequence that we are interested in calculating.

There is a need to avoid zeroes on the unit circle. This problem can be overcome by first multiplying the input sequence  $x(n)$  with the following exponential sequence:

$$x_{\alpha}(n) = \begin{cases} \alpha^n x(n) & n = 0, \dots, N-1 \\ 0, & n = N, \dots, L-1 \end{cases} \quad \text{with } L \gg 8N, \quad (15)$$

where  $\alpha < 1$  and  $\alpha \cong 1$ . This step causes the radius of its zeroes scaled down by the factor  $\alpha$ , moving them slightly inside the unit circle (Pei and Lin, 2006). Also, even though the sequence is finite, its cepstrum sequence is still infinite (Oppenheim and Schaffer, 2009). To reduce the aliasing effect, we need to add trailing zeroes to  $\alpha^t x(n)$ , as in Equation 15 (Pei and Lin, 2006).

### Minrceps algorithm

1. Choose a value  $\alpha \leq 1$  and  $\alpha \cong 1$  to move the zeroes slightly inside the unit circle as in Equation 15.
2. Perform an  $L$ -point FFT on  $x_{\alpha}(n) = \alpha^n x(n)$ , where  $n = 0, 1, \dots, (N-1)$ , to get  $X_{\alpha}(k)$ ,  $k = 0, 1, \dots, (L-1)$ , where  $L \gg 8N$ .
3. Perform an IFFT on  $\ln |X_{\alpha}(k)|$  to get  $\hat{h}_{\alpha}(n)$ , which is equal to  $\hat{h}_{\alpha,min}(n)$ .
4. Construct  $\hat{c}_{\alpha,min}(n)$  from  $\hat{h}_{\alpha,min}(n)$  using Equation 8.
5. Calculate  $x_{\alpha,min}(n)$  from  $\hat{c}_{\alpha,min}(n)$  using the recursion formula in Equation 7.
6. Rescale  $x_{\alpha,min}(n)$  to get  $x_{min}(n) = x_{\alpha,min}(n)\alpha^{-n}$ .  
Pei and Lin (2006).

## TEST EXAMPLES

We implemented the `minrceps` algorithm presented in the previous section using Octave, a MATLAB-like environment (Eaton et al., 2013). We test four cases to demonstrate the suitability of the algorithm. We plot a comparison of the input and output signals, as well as their amplitude and phase spectra respectively. We use pole-zero plots to illustrate whether or not the signal in question is minimum-phase using the classic system definition. In this regard, we consider the signal values to represent filter coefficients of a system, comprising the numerator of the rational transfer function. We set the denominator to one, which results in a single pole at the origin. Finally, we compute the absolute difference between the minimum phase reconstruction using our "minrceps" method and a reconstruction of the output using the Hilbert transform of the amplitude spectrum (Quatieri and Oppenheim, 1981).

Our four test cases are summarized as follows:

**Case A:** Minimum phase wavelet

**Case B:** Mixed-phase wavelet with linear phase

**Case C:** Mixed-phase wavelet with linear phase and a number of isolated zeroes in the amplitude spectrum

**Case D:** Mixed-phase wavelet with linear phase and an interval of zeroes in the amplitude spectrum

For the Case A, we generate a minimum-phase seismic wavelet using the `wavemin` function in the CREWES toolbox (Margrave, 2001). The input parameters are given in Table 1. Cases B-D have the same parameters as Case A, and we use the amplitude spectrum from Case A as a starting point for all four cases. In Case B, we generate a linear phase spectrum and combine it with the amplitude spectrum from Case A to generate our input signal. In Case C, we start with the linear phase spectrum from Case B and we take the amplitude spectrum from Case A, zeroing out five values in non-adjacent locations to create isolated zeros. Case D is similar to Case C, but this time we zero out an interval of five values in the amplitude spectrum to generate our input signal. For the `minrceps` algorithm, we set the values of the parameters  $\alpha$  and  $L$  to be 0.9999 and 24 respectively.

| Parameter | $f_{dom}$ | $dt$ | $ns$        | $lt$   |
|-----------|-----------|------|-------------|--------|
| Value     | 30Hz      | 4ms  | 128 samples | 0.508s |

Table 1. Parameters of input wavelets used to test `minrceps` algorithm

### Minimum-phase input (Case A)

This first test case represents the "do nothing" case - we would expect that the `minrceps` algorithm would not modify a minimum-phase input. In Figure 1 we see that the output

signal, amplitude spectrum, and phase spectrum are nearly identical. Looking at pole-zero plots of the input and output in Figure 2, we see little to no change in the location of zeroes. Finally, looking at the difference between the *minrceps* output and a Hilbert transform reconstruction in Figure 3, we see that there is a very small absolute difference between the two, with a maximum percentage difference on the order of magnitude of 1%. This is likely due to the bandlimited nature of the input, and possibly accumulation of rounding errors as well. We conclude that the algorithm successfully passes the "do nothing" case.

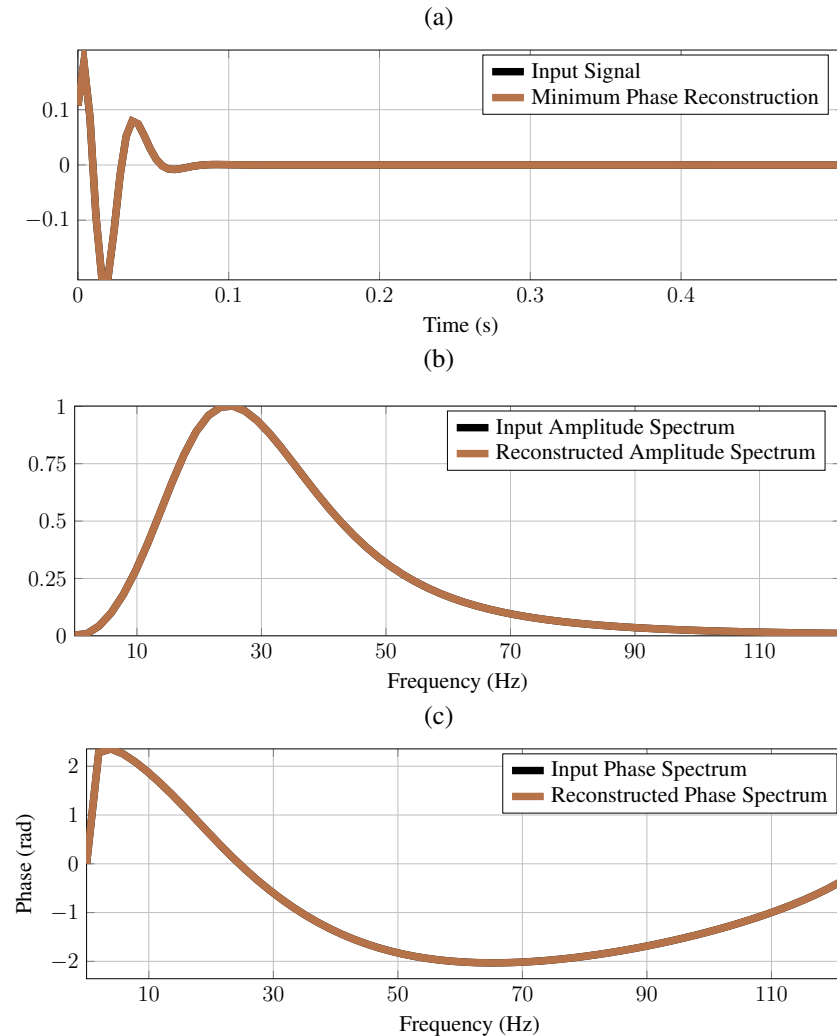


FIG. 1. Case A: Minimum phase input. (a) Input signal and minimum phase reconstruction generated using *wavemin* and *minrceps* respectively. (b) Amplitude spectra of input and output. (c) Phase spectra of input and output. The curves are so close in value that they appear to lie on top of one another.

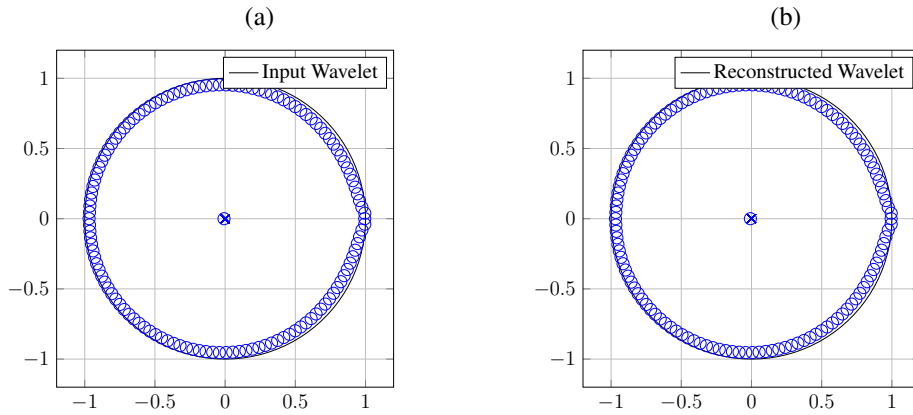


FIG. 2. Case A: Pole-zero plots showing location of poles and zeroes of signal. Poles are denoted by x's and zeros by o's. (a) Input signal. (b) Minimum-phase reconstruction using minrceps algorithm.

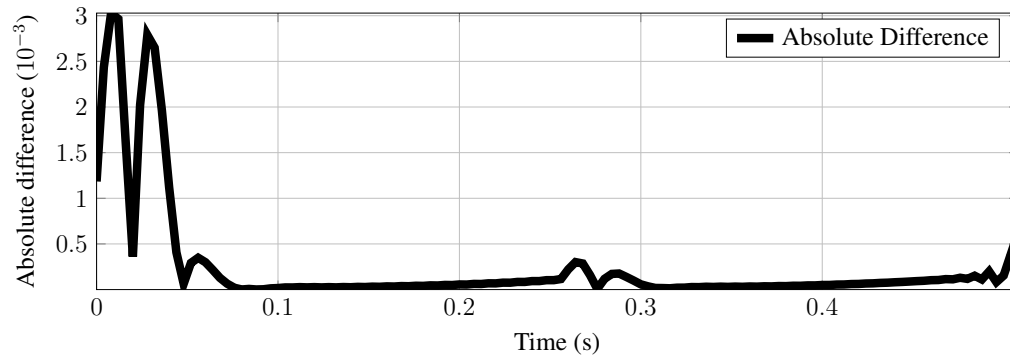


FIG. 3. Case A: Absolute difference between output signal shown in Figure 1a and a minimum phase reconstruction of the minrceps output using a Hilbert transform reconstruction method.

### Mixed (linear) phase input (Case B)

The second test case has the same amplitude spectrum as Case A, but we apply a linear phase to delay the energy of the signal - giving a mixed phase input. Figure 4a shows that the algorithm has shifted the energy of the output signal to the beginning of the signal with an identical shape to the minimum phase input in 1a. We also note no change in the amplitude spectrum, which is desired property (Figure 4b). In Figure 4c, we observe the linear phase of the input vs. the phase spectrum of the minimum phase reconstruction which is near zero in comparison. The pole-zero plots in Figure 5 show that the minrceps output has visibly placed the zeroes inside the unit circle, making the output minimum phase by the pole-zero definition. Note that the pole-zero plot for the reconstructed signal in Case B (Figure 5b) is slightly different from either pole-zero plot in Case A (Figure 2). Looking at the difference between our minrceps output and a Hilbert transform reconstruction of itself in Figure 6, we see that the absolute difference on average between the two is actually smaller than in Case A by about an order of magnitude. This is an interesting result, but acceptable nonetheless as errors are still very small between the minrceps and Hilbert transform reconstructions.

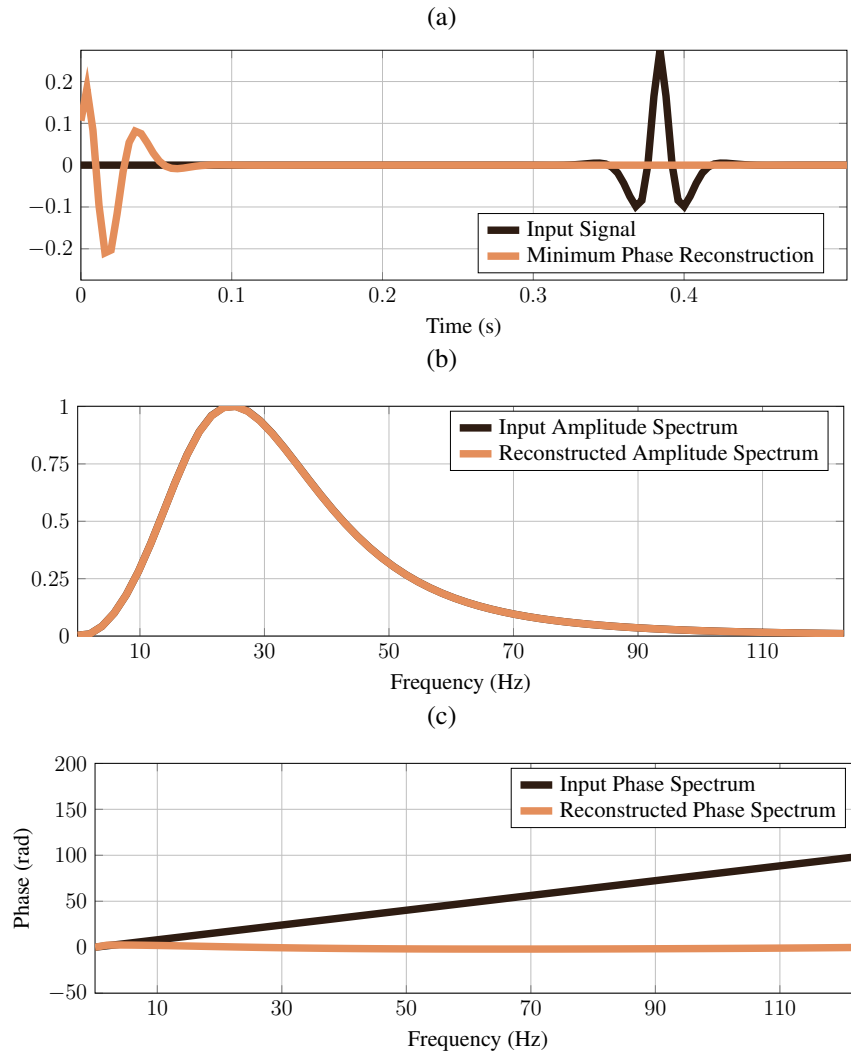


FIG. 4. Case B: Mixed (linear) phase input. (a) Input signal generated using amplitude spectrum from Figure 1b and applying a linear phase. (b) Amplitude spectra of input and output. (c) Phase spectra of input and output.

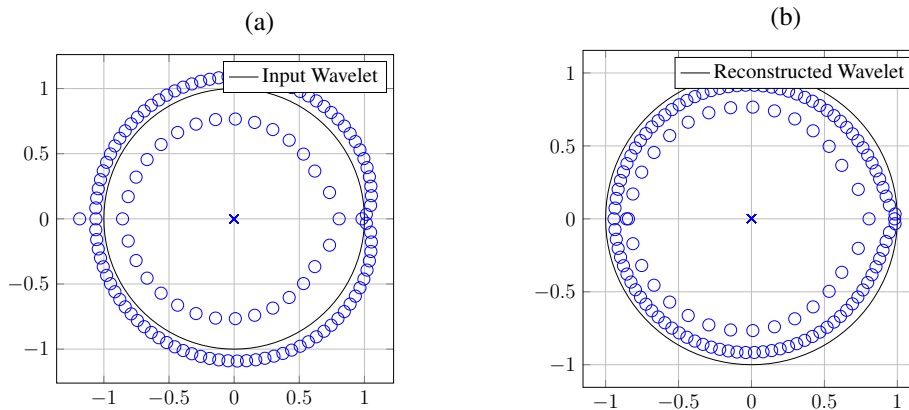


FIG. 5. Case B: Pole-zero plots showing location of poles and zeroes of signal. Poles are denoted by x's and zeroes by o's. (a) Input signal. (b) Minimum phase reconstruction using minrceps.

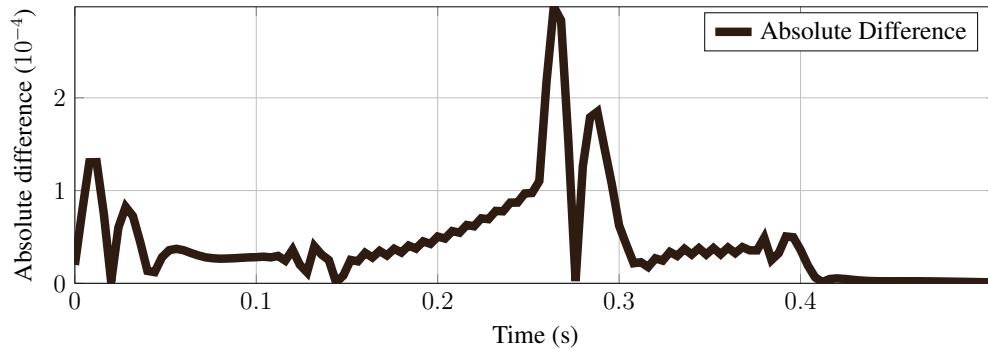


FIG. 6. Case B: Absolute difference between output signal shown in Figure 4a and a minimum phase reconstruction of the *minrceps* output using the Hilbert transform.

### Mixed (linear) phase input with isolated zeroes (Case C)

The final two test cases aim to test the issue of zeroes in the amplitude spectrum of the input. In Case C, we begin with the same amplitude and phase spectra as Case B (Figure 4), but add five isolated zeroes to the amplitude spectrum of the input (Figure 7). We see in Figure 7a that the *minrceps* output has front-loaded energy, although there is now later-time ringing. Looking at the amplitude spectra of the input and the output, we note that the algorithm has begun to fill in the zeroes. The notches in the output at about 10, 50, 85, and 95 Hz are all now non-zero, with no effect on the zero at 40 Hz. A new notch at about 30 Hz is created that was not in the input. The pole-zero plots in Figure 8 show that the *minrceps* output appears to be minimum-phase by the classic definition, with all poles and zeroes within the unit circle. Looking at the difference between our *minrceps* output and a Hilbert transform reconstruction in Figure 9, we see larger absolute differences by about an order of magnitude than in Cases A or B.

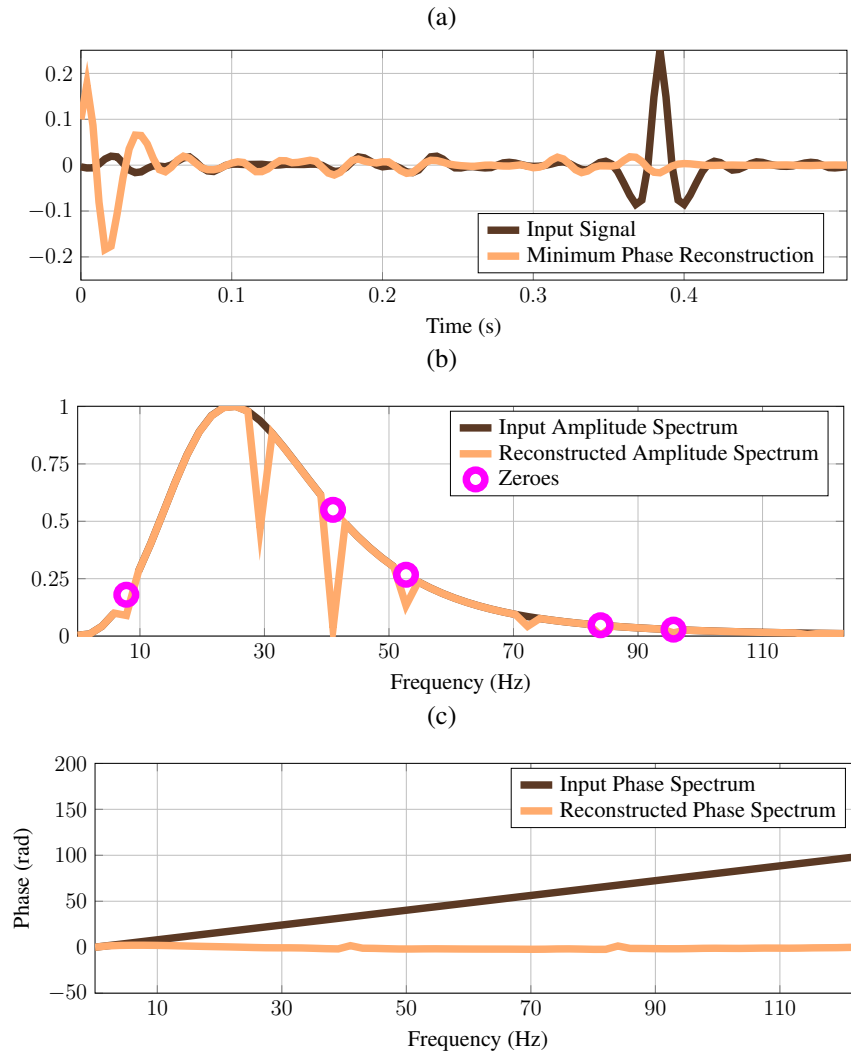


FIG. 7. Case C: Mixed (linear) phase input with isolated zeroes. (a) Input signal generated using phase spectrum from Figure 4c, and amplitude spectrum from Figure 1b with a number of isolated zeros introduced. (b) Amplitude spectra of input and output, with isolated zeroes in input spectrum shown in magenta circles. (c) Phase spectra of input and output.

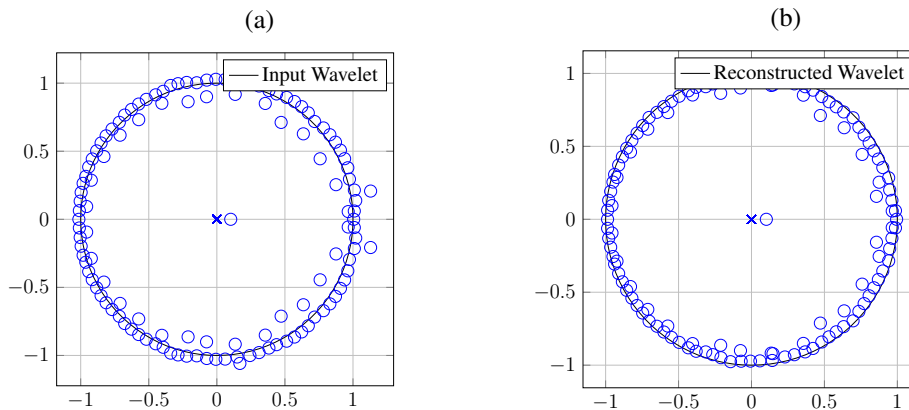


FIG. 8. Case C: Pole-zero plots showing location of poles and zeroes of signals. Poles are denoted by x's and zeroes by o's. (a) Input signal. (b) Minimum phase reconstruction using minrceps.

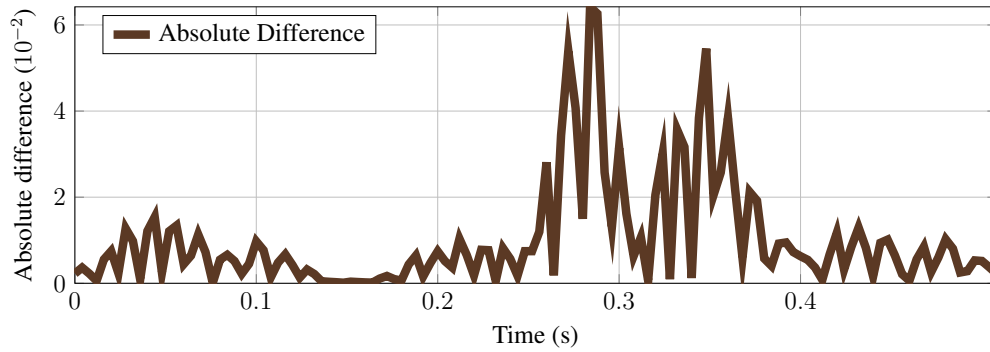


FIG. 9. Case C: Absolute difference between output signal shown in Figure 7a and a minimum phase reconstruction of the *minrceps* output using a Hilbert transform reconstruction.

### Mixed (linear) phase input with interval of zeroes (Case D)

The final test, Case D, is an extension of Case C but with an interval of zeroes in the input amplitude spectrum instead of isolated zeroes (Figure 10b). This case gives the worst result visually, with the energy in the output appearing less front-loaded than any of the other cases along with the ringing observed in Case C (Figure 10a). When we look at the amplitude spectra, we see that the algorithm has again compensated for the zeroes. There is still an interval from about 12-15 Hz in the output that is still near-zero. This is likely the result for the visible worse result. Looking at the difference between our *minrceps* reconstruction and a Hilbert transform reconstruction in Figure 12, we see a similar magnitude of error as that with the isolated zeroes in Case C. Even with the visibly worse result, we note that the pole-zero plots in Figure 11 show that all poles and zeroes appear to still be within the unit circle.

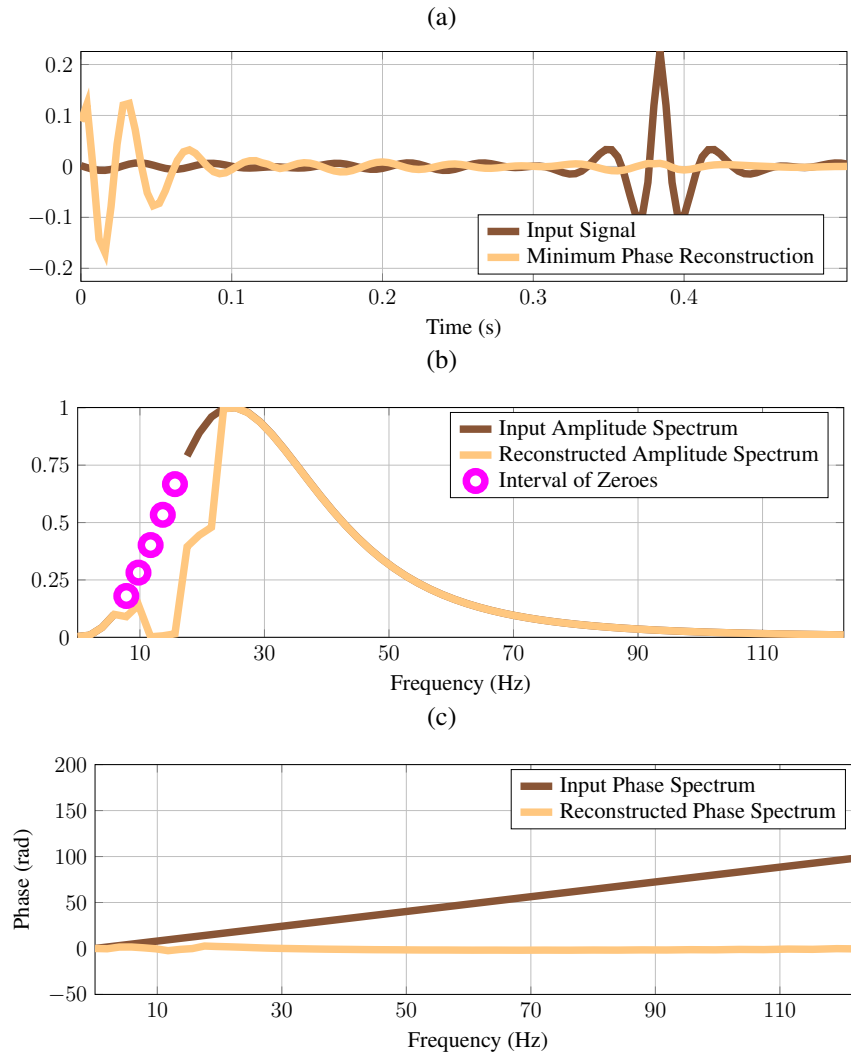


FIG. 10. Case D: Mixed (linear) phase input with interval of zeros. (a) Input signal generated using phase spectrum from Figure 4c, and amplitude spectrum from Figure 1b with an interval of zeros introduced. (b) Amplitude spectra of input and output, with interval of zeroes in input spectrum shown in magenta circles. (c) Phase spectra of input and output.

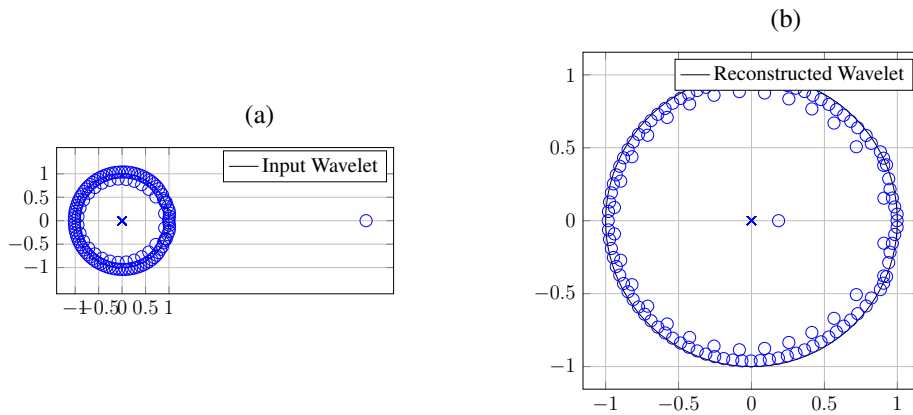


FIG. 11. Case D: Pole-zero plots showing location of poles and zeroes of signals. Poles are denoted by x's and zeros by o's. (a) Input signal. (b) Minimum phase reconstruction using *minrceps*.

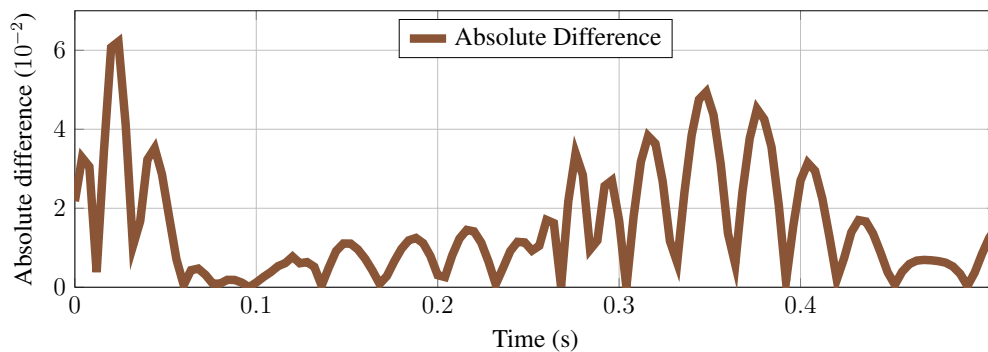


FIG. 12. Case D: Absolute difference between output signal shown in Figure 10a and a minimum phase reconstruction of the *minrceps* output using a Hilbert transform reconstruction.

### Algorithm Performance

In cases A-D, we tested the performance of the *minrceps* algorithm which was used to convert the signals to a minimum-phase equivalent with the same amplitude spectrum. We observed in the case of a minimum-phase input (Case A), the algorithm essentially does not change the signal. In Case B, we saw that the algorithm successfully converted a linear phase input with a well-behaved amplitude spectrum to minimum phase. Even when we added zeroes to the amplitude spectrum with linear phase in an isolated sense (Case C), the result appears very similar to the output from Case B. When applying an interval of zeroes to the amplitude spectrum with linear phase input in Case D, we get a result that does not appear visibly to have as much of its energy front-loaded as the other three cases. However, a pole-zero plot shows that it still appears to nearly satisfy the classic definition of minimum phase. When we zero out parts of the input amplitude spectra as in cases C and D, we observe ringing as well as the output amplitude spectrum not matching the input. The ringing in the output is likely due to the zeroing of the input amplitude spectra and is not caused by the application of the algorithm itself.

In addition to testing different cases where we have signals with ill-conditioned ampli-

tude spectra, we also need to consider the effect of altering or modifying the parameters  $\alpha$  and  $L$ . This could be especially important for improving results with problematic spectra, such as Case D.

## DECONVOLUTION TEST

Since we want to use the minrceps algorithm for analysis of geophysical and related signals, we test its suitability in generating minimum phase outputs by a simple deconvolution test. We take each minimum-phase reconstruction from the previous section as a source wavelet (Figure 13a) and convolve it with a synthetically-generated white reflectivity (Figure 13b). We then perform a simple stationary Wiener deconvolution to return the reflectivity where we use the input trace itself as the design trace, number of lags equal to the length of the wavelet, and a stability factor of 0.1. In Figure 14, we show the resulting seismic traces after convolving the wavelets in Figure 13a with the reflectivity in Figure 13a. The estimated reflectivities from deconvolution for each case along with the original reflectivity are displayed in Figure 15.

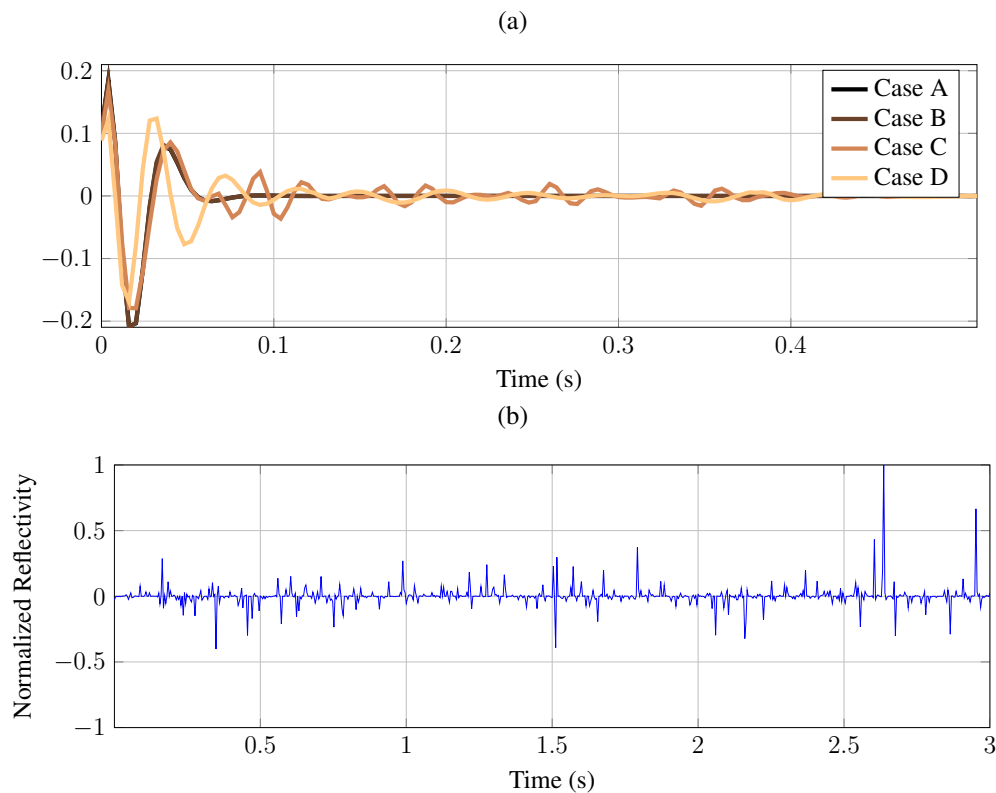


FIG. 13. Deconvolution test inputs. (a) Source wavelets which are outputs from Cases A-D from the previous section, calculated using the minrceps function. (b) Synthetic reflectivity.

We see in Figure 15 that the returned reflectivities for all four cases are very similar. Most significantly, there is not a large noticeable difference in the recovered reflectivity from Case A vs. Case D even though the wavelets appear considerably different (Figure 13a). This suggests that the minrceps algorithm is returning an output that is close enough to meeting the minimum-phase condition to give good deconvolution results, even though its

amplitude spectrum was ill-conditioned.

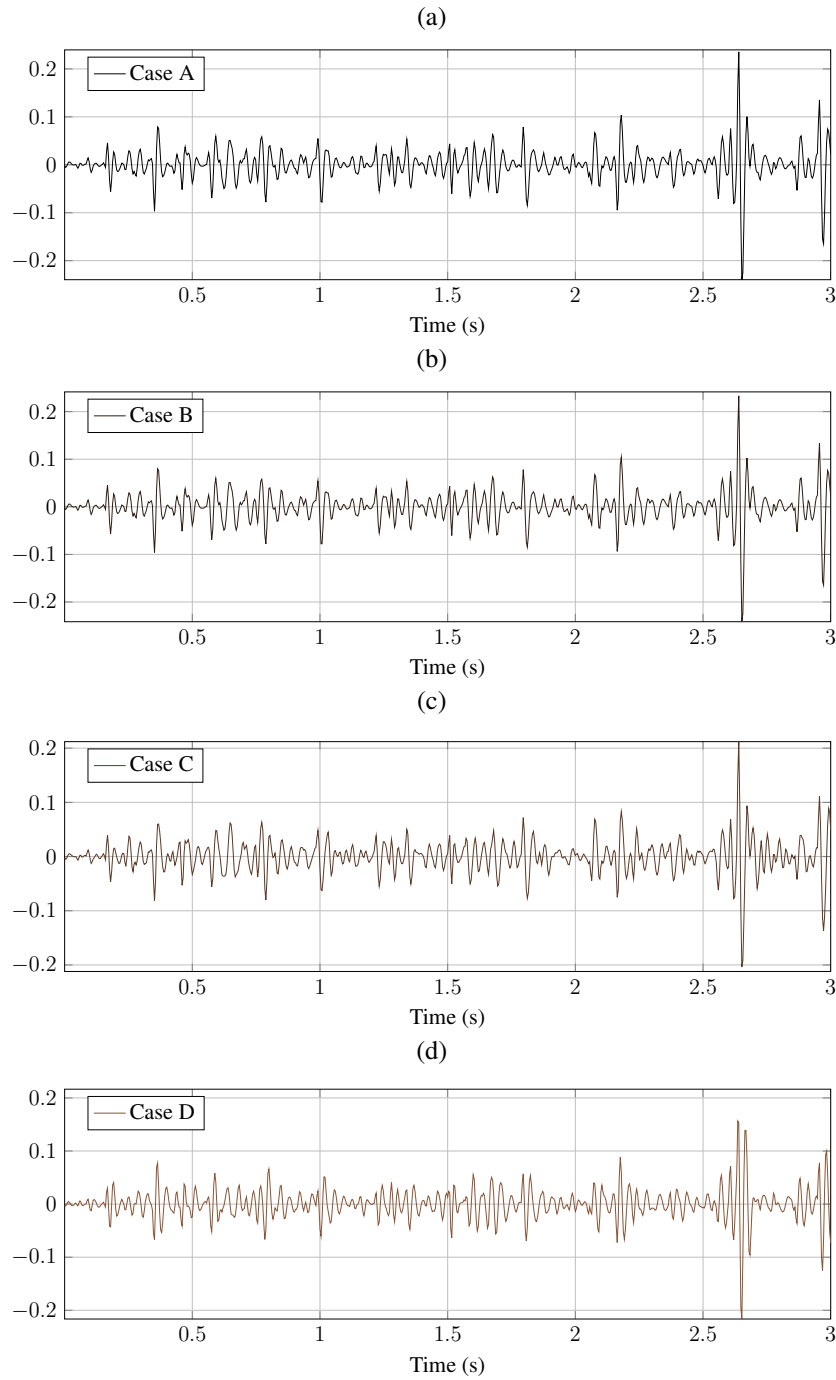


FIG. 14. Seismic traces generated convolving wavelets in Figure 13a with reflectivity in Figure 13b.

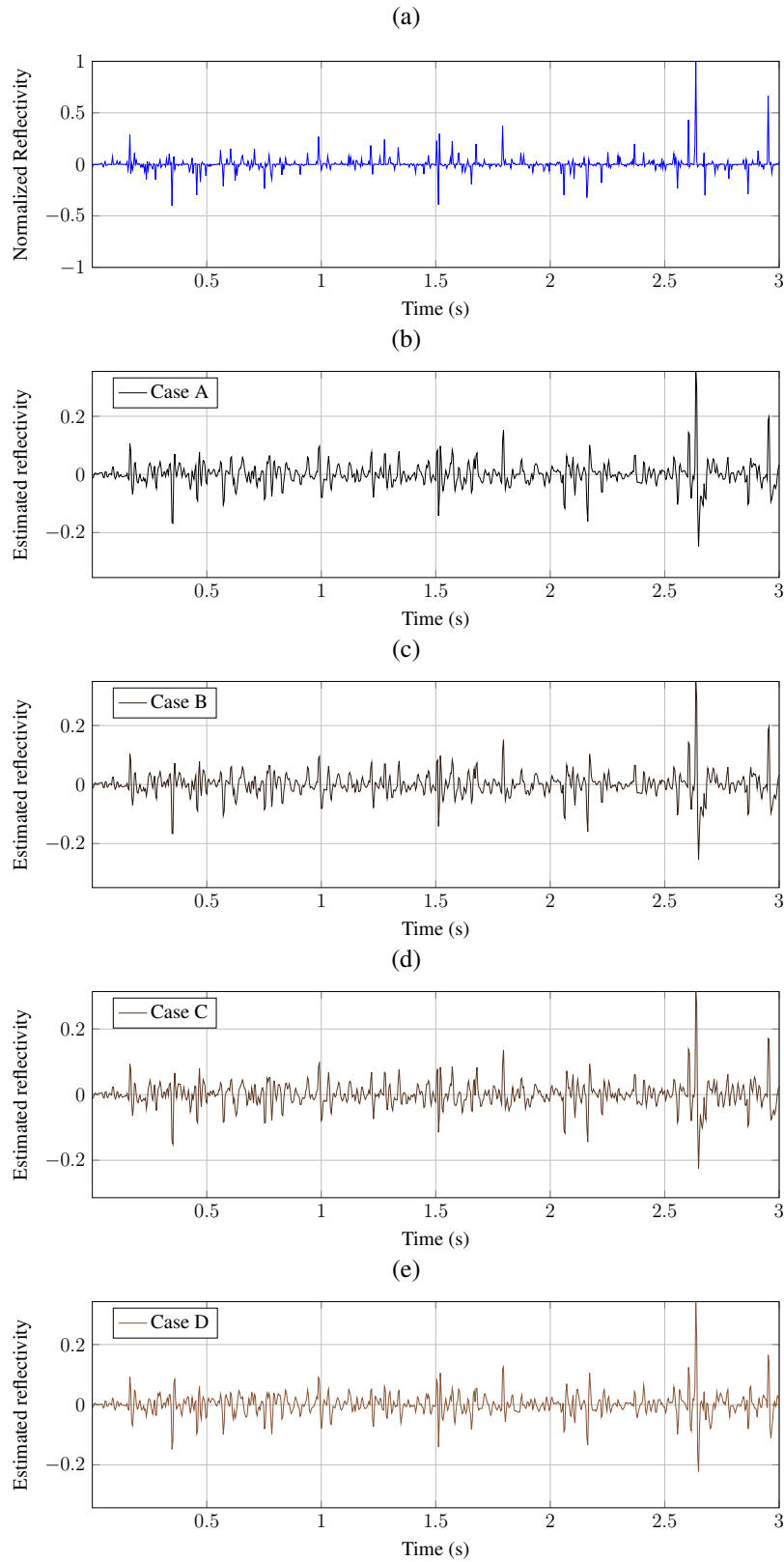


FIG. 15. Original reflectivity (a) along with reflectivities estimated from stationary Wiener deconvolution of the seismic traces in Figure 14 (b-e).

## MINIMUM PHASE METRIC

We have shown the `minrceps` algorithm gives signals close enough to minimum phase to get good deconvolution results. Since we are looking at *signals* that can only be described minimum phase approximatley, we propose two measures to quantitatively describe their "minimum phaseness", or how close they are in fact to being minimum phase. Eventually, we hope to gain some idea of how accurate (or inaccurate) a certain geophysical process, like deconvolution is based on how strongly our source wavelet violates the minimum-phase criterion. Our methods originate with the systems definition of minimum phase, namely poles and zeroes. Our metrics take into account both the number of poles and zeroes on or outside the unit circle, and the average distance from the unit circle of those poles and zeros that are located outside it.

### Pole-Zero Ratio

We call our first metric the Pole-Zero Ratio (PZR). It is simply the ratio of the number of zeroes and poles of a system/signal that lie on or outside the unit circle on the complex plane to the total number of zeroes and poles. For example, a system with a poles at  $z = \pm 2i$  and a zero at  $z = -0.5$  would have a PZR of  $2/3$ , because two-thirds of the total poles and zeroes of the system lie on or outside the unit circle  $|z| = 1$ . It follows from this that a minimum-phase signal/system would have a PZR of 0, because all poles and zeros by definition are inside the unit circle. The corollary of this is that maximum-phase sequences will have a PZR of 1, because all of their poles/zeros either lie on or outside the unit circle. We would assume that the smaller the PZR, the closer the signal is to minimum phase.

### Pole-Zero Distance

Our second metric is named the Pole-Zero Distance (PZD). It is a measure of the average distance of all of the poles and zeroes *on or outside* the unit circle from the unit circle itself. For example, if all of the poles and zeroes of a sequence were located on the unit circle, the PZD would return a value of zero. If all of the poles and zeroes are located inside the unit circle (minimum phase), we give it a dummy value of  $-1$ . In the previous example of two poles at  $z = \pm 2i$  and a zero at  $z = -0.5$ , we would calculate a PZD of 1,

$$PZD = \frac{\sum_{(|P/Z| \geq 1)} (|P/Z| - 1)}{(\text{Number of P/Z outside } |z| = 1)} = \frac{(2 - 1) + (2 - 1)}{(2)} = 1.$$

With the PZD, we would potentially expect a larger number to represent a larger deviation from minimum phase. However, this measure may be skewed by isolated poles and zeroes lying well outside the unit circle.

### Metric test

We apply these metrics to the four cases looked at previously: minimum-phase input, linear phase input, linear phase with isolated zeroes in amplitude spectrum, and linear phase

with interval of zeroes (Figures 1a), 4a), 7a), and 10a) respectively. The results for the PZR and PZD calculations for each case, as well as ratios for the outputs from the minrceps algorithm are listed in Table 2.

|               | Input | PZR    | PZD    | Output | PZR    | PZD    |
|---------------|-------|--------|--------|--------|--------|--------|
| <b>Case A</b> |       | 0      | -1     |        | 0      | -1     |
| <b>Case B</b> |       | 0.7559 | 0.0855 |        | 0      | -1     |
| <b>Case C</b> |       | 0.7559 | 0.0493 |        | 0      | -1     |
| <b>Case D</b> |       | 0.7402 | 0.0568 |        | 0.0472 | 0.0020 |

Table 2. Values of PZR and PZD calculated for the inputs and outputs used to test the minrceps algorithm.

We see that in the Case A input, we have a PZR of zero and a PDZ of  $-1$ . This is what we would expect, as Case A represents a minimum-phase wavelet. There is a drop in the PZR in Case B, where about 25% of the poles/zeroes now lie on or outside the unit circle. Similar values can be seen for Cases C and D. This drop is a result mainly of applying a linear phase to the data. It is interesting to note that the addition of isolated zeroes to the amplitude spectrum as in Case C did not lower the PZR from case B (with a complete amplitude spectrum), but introducing an interval of zeroes as in Case D did cause a slight drop in the PZR (making it closer to being minimum phase). With regards to PZD, we notice that the Case B input has the highest value. If we compare Figures 5a and 8a, we notice that although there are several poles in Case C that are further out from the unit circle, the cluster of poles outside in Case B is on average further away. In our output signals, we notice that Cases A-C are all exactly minimum phase and Case D is very close, likely with one or two zeroes still on or outside the unit circle. From this limited analysis, it is difficult to determine which metric better indicates "minimum phaseness". More tests are required along with a more robust quantitative measurement of how "good" our deconvolution results are to determine this.

## CONCLUSIONS

In this report, we examined an algorithm to convert a signal of arbitrary phase to its minimum phase equivalent. The minrceps algorithm is based upon calculation of the real cepstrum, and has advantages to other Hilbert transform based minimum phase conversion algorithms. We tested the performance of this algorithm on four test cases, incorporating ill-conditioned inputs. The algorithm appears to be able to handle these. The outputs were all found to very close to minimum phase by the classic definition from digital filtering. A simple stationary deconvolution test reveals that the outputs were all close enough to minimum phase that statistical deconvolution was able to return relatively accurate estimates of reflectivity. Finally, we introduced two simple metrics to measure quantitatively how close a signal is to being minimum phase: the Pole-Zero Ratio (PZR) and the Pole-Zero Distance (PZD), and preliminary calculation of these in the test cases indicates more analysis is required to get a better measure of how close a signal is to being minimum phase using these metrics.

## **Future Work**

The minrceps algorithm is an alternative to other Hilbert transform minimum-phase reconstruction methods, and there is a possibility that the process can be linearized as it does not require a separation and recombination of the phase and amplitude spectra of the signal in question. We would like to investigate this possibility. Also, we need to develop a better metric to quantitatively assess the deconvolution results vs. an input reflectivity. Finally, in relation to the aforementioned desire to better quantify deconvolution results, we would like to analyze deconvolution performance vs. PZR and PZD to better constrain which is a better measure of minimum phaseness.

## **ACKNOWLEDGEMENTS**

We thank the sponsors of CREWES for their support. We also gratefully acknowledge support from NSERC (Natural Science and Engineering Research Council of Canada) through the grant CRDPJ 379744-08.

## REFERENCES

- Benesty, J., Sondhi, M. M., and Huang, Y., 2008, Springer handbook of speech processing: Springer.
- Bogert, B. P., Healy, M. J. R., and Tukey, J. W., 1963, The quefrency analysis of time series for echoes: Cepstrum, pseudo autovariance, cross-cepstrum and saphe cracking, *in* Rosenblatt, M., Ed., Time Series Analysis, chap. 15, Wiley, 209–243.
- Bourqui, J., Sill, J. M., and Fear, E. C., 2012, A prototype system for measuring microwave frequency reflections from the breast: *Journal of Biomedical Imaging*, **2012**, 9.
- Eaton, J. W., Bateman, D., Hauberg, S., and Wehbring, R., 2013, GNU Octave: A high-level interactive language for numerical computations - Edition 3 for Octave version 3.8.0.
- Fear, E. C., Li, X., Hagness, S. C., and Stuchly, M. A., 2002, Confocal microwave imaging for breast cancer detection: Localization of tumors in three dimensions: *Biomedical Engineering, IEEE Transactions on*, **49**, No. 8, 812–822.
- Gurbuz, A. C., McClellan, J. H., and Scott, W. R., 2009, A compressive sensing data acquisition and imaging method for stepped frequency gprs: *Signal Processing, IEEE Transactions on*, **57**, No. 7, 2640–2650.
- Herrmann, O., and Schuessler, W., 1970, Design of nonrecursive digital filters with minimum phase: *Electronics Letters*, **6**, No. 11, 329–330.
- Jol, H. M., 2008, Ground penetrating radar theory and applications: Elsevier.
- Karl, J. H., 1989, An Introduction to Digital Signal Processing: Academic Press Professional, Inc.
- Lamoureux, M. P., Gibson, P. C., and Margrave, G. F., 2011, Minimum phase and attenuation models in continuous time: CREWES Research Report, **23**.
- Lamoureux, M. P., and Margrave, G. F., 2007a, An analytic approach to minimum phase signal: CREWES Research Report, **19**.
- Lamoureux, M. P., and Margrave, G. F., 2007b, A band-limited minimum phase calculation: CREWES Research Report, **19**.
- Lamoureux, M. P., and Margrave, G. F., 2007c, A minimum-phase, band-limited delta spike: CREWES Research Report, **19**.
- Margrave, G. F., 2001, Numerical methods of exploration seismology with algorithms in matlab: The University of Calgary Publ.
- Margrave, G. F., 2013, Goph 517 - methods of seismic data processing: course lecture notes.
- Margrave, G. F., Lamoureux, M. P., and Henley, D. C., 2011, Gabor deconvolution: Estimating reflectivity by nonstationary deconvolution of seismic data: *Geophysics*, **76**, No. 3, W15–W30.
- Mian, G. A., and Nainer, A., 1982, A fast procedure to design equiripple minimum-phase fir filters: *Circuits and Systems, IEEE Transactions on*, **29**, No. 5, 327–331.
- Oppenheim, A. V., 1965, Superposition in a class of nonlinear systems: Ph.D. thesis, Massachusetts Institute of Technology.
- Oppenheim, A. V., and Schaffer, R. W., 2009, Discrete-Time Signal Processing: Prentice Hall Press.
- Pei, S.-C., and Lin, H.-S., 2006, Minimum-phase fir filter design using real cepstrum: *Circuits and Systems II: Express Briefs, IEEE Transactions on*, **53**, No. 10, 1113–1117.
- Quatieri, T. F., Jr, and Oppenheim, A. V., 1981, Iterative techniques for minimum phase signal reconstruction from phase or magnitude: *Acoustics, speech, and signal processing, IEEE Transactions on*, **ASSP-29**, No. 6, 1187–1193.

- Robinson, E. A., 1967, Predictive decomposition of time series with application to seismic exploration: *Geophysics*, **32**, No. 3, 418–484.
- Robinson, E. A., and Treitel, S., 1967, Principles of digital wiener filtering: *Geophysical Prospecting*, **15**, No. 3, 311–332.
- Sherwood, J., and Trorey, A., 1965, Minimum-phase and related properties of the response of a horizontally stratified absorptive earth to plane acoustic waves: *Geophysics*, **30**, No. 2, 191–197.
- Stathaki, T., and Fotinopoulos, I., 2001, Equiripple minimum phase fir filter design from linear phase systems using root moments: *Circuits and Systems II: Analog and Digital Signal Processing, IEEE Transactions on*, **48**, No. 6, 580–587.
- Yilmaz, Ö., 2001, *Seismic data analysis, vol. 1: Society of Exploration Geophysicists Tulsa.*
- Ziolkowski, A., and Bokhorst, K., 1993, Determination of the signature of a dynamite source using source scaling, part 2: Experiment: *Geophysics*, **58**, No. 8, 1183–1194.